JOURNAL OF OPTOELECTRONICS AND ADVANCED MATERIALS Vol. 15, No. 11-12, November - December 2013, p. 1346 - 1351

Influence of the type of carbon nanocharges on the dielectric, mechanical and electroactive properties of polyurethane composites films

L. SEVEYRAT[a], L. LEBRUN[a], M. HEDI JOMAA[a], B. K. WONGTIMNOI[c], Q. LIU[a], B. GUIFFARD[d], K. MASENELLI-VARLOT[b], J. Y. CAVAILLE[b], D. GUYOMAR[a]

[a]*Laboratoire de Génie Electrique et Ferroélectricité, LGEF EA682 INSA Lyon, Bat. Gustave Ferrié, 8 rue de la Physique, F-69621 Villeurbanne Cedex, France*

[b]*MATerials EngIneering and Science (MATEIS), INSA Lyon, CNRS-UMR 5510, Bat. Blaise Pascal, 7 avenue Jean Capelle, F-69621 Villeurbanne Cedex, France*

[c]*(current address) Ingénierie des Matériaux Polymères (IMP), INSA Lyon, CNRS-UMR 5223, Bat. Jules Verne, 17 avenue Jean Capelle, F-69621 Villeurbanne Cedex, France*

[d]*(current address) IETR UMR CNRS 6164, Université de Nantes, 2 rue de la Houssinière, BP 92208, F-44322 Nantes cedex 3, France*

Composites based on a polyurethane polymer matrix filled with various amounts of different types of nano-objects (carbon black, carbon nanotubes and graphene) were prepared and characterized. Such semi-crystalline polymers are very attractive for electromechanical applications as they can generate high strain levels under moderate electrical fieds. The use of conductive fillers is of a great interest because they effectively increase the electromechanical capabilities due to the enhanced relative permittivity. The dielectric constants of the nanocomposite films are presented with the help of the percolation theory and the critical exponents are discussed. It was found that the percolation thresholds depend on the size and shape of the nano-objects. Electromechanical capabilities of the nanocomposite films have been assessed by measuring the thickness strain under applied electric fields at low frequency with a laser interferometer. All composite films showed an improved electromechanical response as compared to the pure polymer.

(Received September 28, 2013; accepted November 7, 2013)

Keywords: Electroactive polymers, Nanocomposites films, Carbone, Conductive nanofillers, Dielectric permittivity, Electromechanical properties

1. Introduction

Electromechanical properties in polymers can be employed to create a large number of sensors and actuators [1,2]. Electroactive polymers (EAPs) have the capability to change their size due to the electrostrictive and Maxwell effects, which are a quadratic function of the applied electric field. Even if the electromechanical coupling is relatively weak for polymers, they can generate high strains. In addition, they present properties of flexibility, ease of processing in different shapes with larges surfaces and low costs. Among the various EAPs, Polyurethane (PU) elastomers are of great interest due to the significant electrical-field strains [3,4].

The total strain is a combination of electrostriction and Maxwell strains, see Equation (1) [5]

$$S = S_{electrostriction} + S_{Maxwell} = M_{33}^{*} E^2 \qquad (1)$$

The Maxwell stress effect comes from the interaction between charges on the electrodes and electrostatic attractions that are due to dielectric inhomogeneities, see Equation (2); from the electrostatic stress it follows a mechanical stress on the electrode and as a consequence a thickness contraction of the polymer.

$$S_{Maxwell} = -\frac{\varepsilon_r^{'} \varepsilon_0}{Y} E^2 \qquad (2)$$

The electrostriction is the change in dimensions of a dielectric material occurring as an elastic strain when an electric field is applied. It is the direct coupling between the polarization and mechanical response in the material. By assuming a linear relationship between the polarization P and the electrical field E, $S_{electrostriction}$ can be expressed by Equation (3).

$$S_{electrostriction} = Q P^2 = Q \varepsilon_0^2 (\varepsilon_r^{'} - 1)^2 E^2 \qquad (3)$$

where Q is the electrostrictive coefficient.

If the deformations due to the Maxwell stress effect account for a negligible part of the total strain, it has been previously published [6,7] that the M_{33} coefficient varies like $(\varepsilon_0 (\varepsilon_r^{'} - 1)^2) / (\varepsilon_r^{'} Y)$.

As seen in these relations, actuation capabilities depend on the dielectric and mechanical properties of the polymer. One way to improve these properties is to mix nano-objets with the polymer matrix. Due to the nanoscale dimensions of these objects, a great change of the properties can be obtained with relatively low amount of fillers. The effect is largely increased with the use of conductive fillers leading to excellent physical properties near the percolation threshold [8]. Composites with carbon nanofillers are good candidates for electroactive systems and many studies on these types of fillers [9,10,11,12,13] have shown different physical properties depending on the sizes and the shapes of the fillers and on their distribution into the polymer matrix.

This paper deals with the influence of carbon based nano-objets as fillers on polyurethanes: carbon black (CB), short multiwalled carbon nanotubes (MWNT) and grahene nanopowders of 60 and 15 nm in diameter (gr60 and gr15). The dielectric properties are presented and discussed with the aid of the percolation theory. Depending on the size and the shape of the fillers, a different dimensional organisation appeared, having a significant influence on the dielectric permittivity values. Some microstructural observations are presented in addition. The Young modulus was determined from strain/stress curves at low levels of deformation. Finally measurements of the thickness strain under an applied electrical field are shown for PU-CB and PU-MWNT. The experimental electromechanical coefficients are discussed with the help of electrostrictive relations.

2. Experimental procedure

The polymer is a polyether based thermoplastic polyurethane (PU), ref Estane 58888 NAT021, Lubrizol, which has a density of 1.13 and a hardness of 88 shore A. The properties of the four types of nanofillers are summarised in Table 1.

The nanocomposite films were prepared using the solution cast method. Before use, the PU granules were heated at 80°C for 3 h as recommended by the purchaser. Then they were dissolved in N,N-DiMethylFormamide (DMF, Sigma-Aldrich D158550, 99%) with a ratio of 40% PU into DMF. The PU-DMF solution was maintained at 80°C for 2 hours. Carbon nanofillers were dispersed into DMF using an ultrasonic processor (Hielsher UP400S, 400W, 24 kHz, 7 mm diameter sonotrode) with the following experimental conditions: 20 min duration, 80% amplitude, 80% pulse. This solution was added to that of the polymer and the resultant mixture was heated at 80 °C for 1 hour under mechanical agitation, until a homogeneous and viscous solution was obtained.

This solution was degassed for 24 hours at room temperature before depositing on glass plate with an Elcometer 3700 doctor blade film applicator. The samples were put in an oven at 60°C for one day then removed from glass. A second heating treatment at 125°C for 3 h was applied in order to eliminate the residual solvent. The thickness of the films was about 50 µm after drying.

Table 1. Properties of the four types of carbon based nanofillers.

Denominations	CB	Gr60	Gr15	MWNT
Details	Carbon black XC72R	Graphene nanopowder	Graphene nanopowder	Short multiwalled carbon nanotubes - 4w% COOH
Purchaser	Cabot corporation	Graphene supermarket	Graphene supermarket	Nanostructured & Amorphous Materials Inc
Diameter (nm)	30	60	15	< 8
Length (µm)	-	3-7	5	0.5-2
Specific area (m2/g)	250	<15	50	380

The dielectric properties were obtained using Schlumberger Solartron 1296 dielectric interface and 1255 impedance analyzer at 1 V over a frequency range from 0.1 Hz to 100 kHz on 25 mm diameter samples with gold electrodes sputtered on both sides.

The microstructural observations on the cryofractures of PU-CB, PU-Gr60 and PU-gr15 were performed using a Zeiss Supra 55VP Scanning Electron Microscope operating under high vacuum, at low accelerating voltage (typically 700 V) and without any gold coating. Images were acquired with the Everhart-Thornley secondary electron detector. Direct observations of the PU-MWNT film surface were performed on a FEI ESEM XL30 FEG from the Centre Lyonnais de Microscopie, under high vacuum and with an acceleration voltage of 30 kV. The film surface was coated with gold to prevent any charging effect. The secondary electron signal was collected with the Everhart-Thornley detector. The fracture surface of the PU-MWNT film was characterised using the same microscope but without any coating, at low accelerating voltage (1 kV).

The Young modulus was determined on 40×15 mm2 samples (coated with gold electrodes), using a Newport platin, at 0.1 Hz by applying a deformation of 2.5%.

The field-induced thickness strain S was measured on 25 mm diameter samples with a double-beam laser interferometer (Agilent 10889B), with a precision in the order of 10 nm. The sample was positioned between two circular electrodes and a mirror was placed on the upper electrode to reflect the laser beam A bipolar electric field (0.1 Hz) was supplied by a function generator (Agilent

33250A) amplified by a factor 1000 through a high-voltage lock-in amplifier (Trek10/10B).

3. Results and discussion

3.1. Dielectric characterization

As the electromechanical capability depends directly on the dielectric constant, the aim is to obtain high values and it is possible just before the percolation threshold in systems with conductive nanofillers [8].

Table 2 presents the various amounts of carbon based fillers which have been tested. The percolation threshold f_c was found to be different for the 4 PU composites films; it was estimated from the dielectric properties which show an abrupt change near the threshold f_c. Indeed, the variation of the dielectric constant ε_r' for $f < f_c$ can be described by the following relation [14,15,16]:

$$\varepsilon_r' = \varepsilon_{rm}' \left(\frac{f_c - f}{f_c} \right)^{-q} \quad (4)$$

where ε_{rm}' is the pure PU dielectric permittivity and q a critical exponent.

In order to check that the percolation theory well describes the dielectric constant versus content variation and in order to estimate the critical component, the logarithm of ε_r' is plotted in function of the logarithm of $(f_c\text{-}f/f_c)$ as shown in Fig. 1.

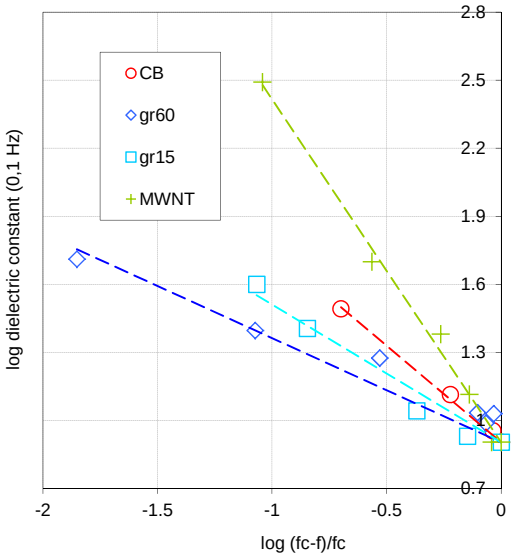

Fig. 1. Evolution of the log of dielectric constant versus the log of $(f_c\text{-}f/f_c)$ showing a linear relation for CB, gr60, gr 15 and MWNT PU composite films.

Table 2. Tested volume fractions, percolation threshold and critical exponent for the 4 PU composites films.

System	PU-CB	PU-Gr60	PU-Gr15	PU-MWNT
Tested volume fractions f (%)	0.1/0.5/1/1.25/ 1.5	0.5/1/1.5/5/6.5/ 7/7.1/7.25/7.5	0.5/1/1.5/1.6/ 1.75/2/2.25	0.1/0.3/0.5/0.8/ 1/1.25/1.5
Percolation threshold f_c (%)	1.25	7.1	1.75	1.1
Critical exponent q	0.85 (3D)	0.46 (3D)	0.61 (3D)	1.51 (2D)

The experimental results are in good agreement with the theoretical law, with a correlation coefficient comprised between 0.97 and 0.99. The q values are reported in table II. According to some authors [17,18], the critical exponent was 1, 1.35 and 0.7 for 1D, 2D and 3D space dimensions, respectively. The PU-CB, PU-Gr60 and PU-Gr15 systems presents a q exponent of about 0.6-0.8, which is close to the universal value for spherically shaped particles.

It appears that the PU-MWNT would better correspond to a 2D system more than 3D, since it exhibits a critical exponent close to 1.5. It seems to be related to a special organization of this type of nanofillers into the polymer host, at least with our processing procedure.

The percolation law equation (4) shows that the dielectric constant versus the amount of fillers is dependent on the space dimension – through the critical exponent q - and on the percolation threshold value f_c. Fig. 2a and 2b show the theoretical evolution.

The evolution of the dielectric constant with the space dimension shows that a 2D system leads to higher values. This is experimentally observed as shown fig. 2c. Indeed, the PU-MWNT films, with a critical exponent corresponding to a 2D organization, exhibit higher values than the PU-CB ones (3D space dimension from the q value) even if both of them have a very similar percolation threshold (respectively 1.1 and 1.25).

The evolution of the dielectric constant with the percolation threshold shows that for a given dielectric constant, the higher the f_c value, the higher the $(f_c\text{-}f)$ term. As a consequence it can be interesting to introduce fillers with high percolation thresholds, which would permit to remain far below f_c and consequently to keep the conductivity at a reasonably low level. Indeed, the composites very close to the percolation threshold show a dramatic increase of the conductivity and lead to unusable materials; on the contrary with a high value of fc, it is easier to control these values of conductivity. An example of this increase is given in Fig. 2d: to obtain a dielectric constant equal to 30, the amount of fillers f is further from the f_c value for PU-gr60 which presents a higher f_c than for CB which percolation threshold is very low.

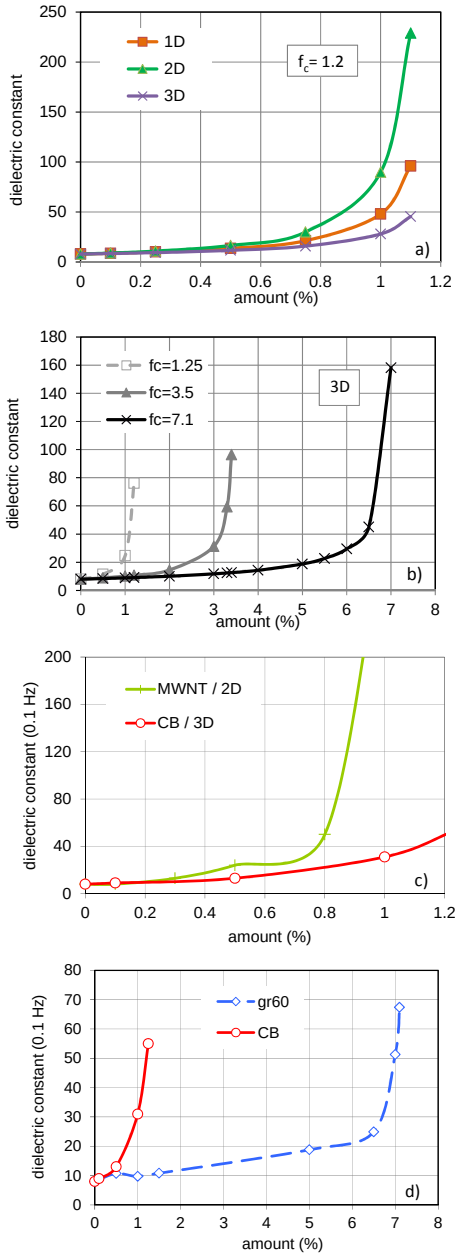

Fig. 2. Evolution of the dielectric constant versus the amount of nanofillers: theoretical estimation from the equation (4) and Stauffer values for the critical exponent with either f_c=1.2 (a) or q=0.7 (b); experimental results at 0.1 Hz for PU-CB and PU-MWNT samples (c), for PU-CB and PU-gr60 samples (d).

3.2. Microstructural characterisation: filler dispersion state

In order to investigate the dispersion of the nanofillers in the polymer matrix, SEM observations have been performed on cryofractured samples of the four types of nanocomposites films. The observations are presented in Fig. 3a to d.

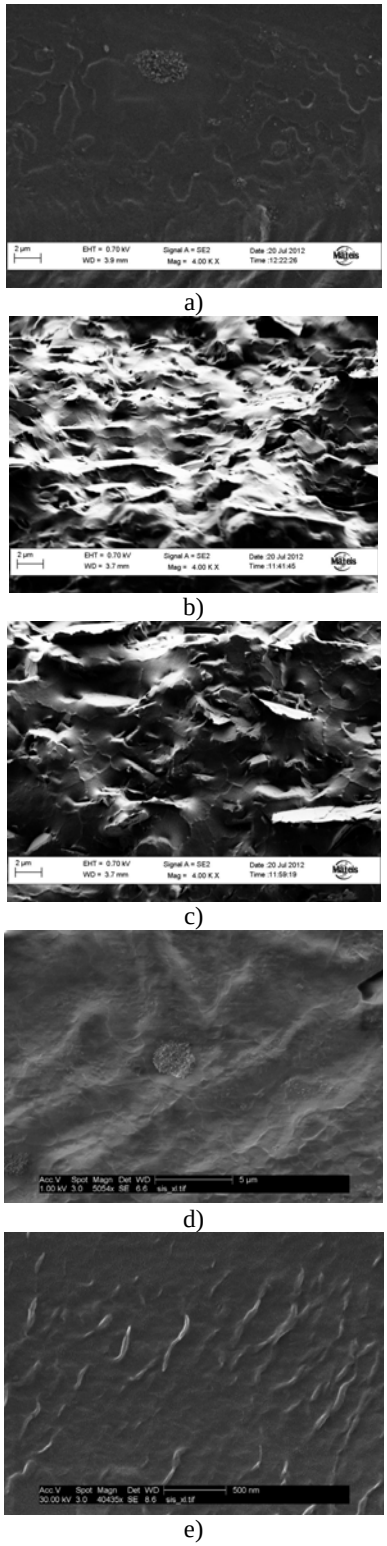

Fig. 3. SEM observations of cryofractured cross-sections of nanocomposites films : a) PU-CB with 1.25 vol% CB, b) PU-gr15 with 1 vol% graphene, c) PU-gr60 with 1 vol% graphene, d) PU-MWNT with 1 vol% MWNTs. e) observation of the PU-MWNT film surface (1 vol% MWNTs).

Fig. 3a shows a fair distribution of carbon black but it can be observed in addition to the individual particles some agglomerates with size smaller than 1 µm. Remembering that the carbon black primary particles and aggregates are spherical, the absence of elongation in the agglomerates is consistent with the 3D dispersion deduced from the dielectric analysis.

As shown in Fig. 3b and 3c, graphene flakes of a few microns long are uniformly dispersed in the polymer without preferential orientation. Indeed in Fig. 3c, some flakes can obviously be observed almost perpendicular to the fracture surface. As for carbon black, this is consistent with the 3D space dimensions.

As far as the PU-MWNT films are concerned, the nanotubes are nicely dispersed, although the cryofracture reveals a few agglomerates (Fig. 3d). Because of their high aspect ratio and the flow direction during processing, the nanotubes are expected to align in the film plane. Thus, a 2D dispersion cannot be deduced from the observation of the fracture surface. Fig. 3e displays an image of the film surface. The nanotubes are clearly visible. Their measured lengths agree well with the nanotube length before incorporation in the matrix. Consequently, it can be concluded that the nanotubes are aligned in the film plane, which corresponds to a 2D space dimension.

3.3. Mechanical properties

Fig. 4 exhibits the experimental results of the Young modulus in function of the filler volume fraction, for the 4 systems. The Young moduli were estimated from the strain/stress curves at low levels of deformation ie 2.5%.

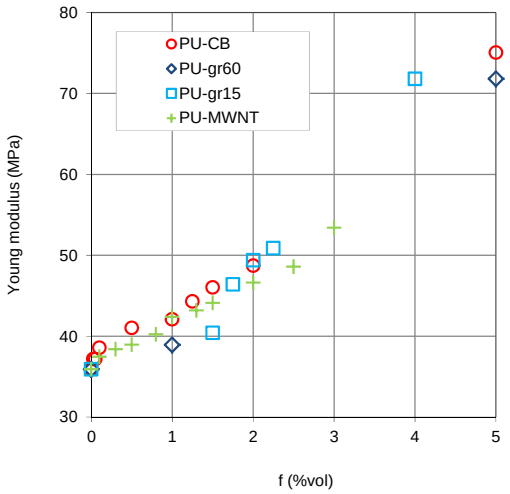

Fig. 4. Evolution of the Young modulus versus the amount of nanofillers for the four nanocomposites films.

The value of Young modulus which is 36 MPa for pure polyurethane films is doubled with 4 or 5 % of nanofillers whatever the shape of the filler. Indeed, for these low volume fractions, it was observed that the filler aspect ratio has in fact only a very slight influence on the composite mechanical properties.

3.4. Electromechanical properties

Fig. 5 exhibits the evolution of the experimental M_{33} coefficient at 4V/µm for PU-CB and PU-MWNT nanocomposite films. This coefficient was calculated from experimental thickness strain divided by the square of the electrical field. In both cases, an optimal value of M_{33} was found for filler contents close to the percolation threshold, somewhat below it. This value of 3 10-15 m2/V2 for the pure polyurethane films is increased by a factor of 2.5 for the optimal nanocomposite films.

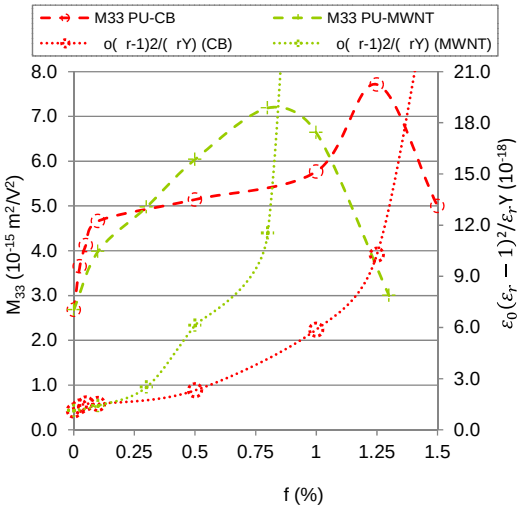

Fig. 5. Evolution of the experimental M_{33} coefficient at 4V/µm and of $(\varepsilon_0 (\varepsilon_r^{'} - 1)^2) / (\varepsilon_r^{'} Y)$ versus filler content for PU-CB and PU-MWNT systems.

$(\varepsilon_0 (\varepsilon_r^{'} - 1)^2) / (\varepsilon_r^{'} Y)$, calculated from experimental permittivity and Young modulus values measured at the same frequency as that used for the electrical field induced strain measurements, are plotted on Fig. 5.

For the lowest volume fractions far from the percolation threshold, the evolution of M_{33} and $(\varepsilon_0 (\varepsilon_r^{'} - 1)^2) / (\varepsilon_r^{'} Y)$ exhibit the same increasing trend. For the highest amounts, $(\varepsilon_0 (\varepsilon_r^{'} - 1)^2) / (\varepsilon_r^{'} Y)$ continues to increase whereas M_{33} decreases.

The relation established by previous authors [6,7] showing a good linearity has been performed on pure polymers without conductive fillers. The measurement of the permittivity of these nanocomposites has been performed at low levels showing a great increase of permittivity close to the percolation threshold. But it is noteworthy that M_{33} has been measured at high electrical field where a decrease or a saturation of the permittivity could be assumed. This point is under investigation. In

addition, measurements of Young Modulus under the same conditions could also provide some explanations.

4. Conclusions

Composites films of 50 µm were elaborated with PU and carbon black (CB), graphene nanoflakes 60 and 15 nm (gr60 and gr15) in diameter and short multiwalled nanotubes functionalized with COOH (MWNT) using the solution cast method. SEM was performed to observe the filler dispersion state in the matrix.

The dielectric properties of the nanocomposites films were all increased with the amount of the fillers and very high values of dielectric constant were obtained just before the percolation threshold f_c. The evolution was found to be different depending on the space dimension and depending on the fc value. Experimental data were in good agreement with the theoretical percolation law. These results are important for the choice of the nanofiller type: better electromechanical performances can be expected with a 2D space dimension system and high percolation thresholds.

The mechanical properties were not really affected by the shape of the nanofillers.

The measurement of the thickness strain under an applied electrical field showed an increase of the electroactive performance; the electromechanical coefficients were compared to the theoretical estimation and a good agreement was obtained but only for filler contents under the percolation threshold.

Acknowledgements

The authors acknowledge the Centre Lyonnais de Microscopie (CLYM) for the access to the FEI ESEM XL30 FEG microscope.

The authors gratefully aknowledge ANR for providing financial support (ANR-2010-INTB-910-01).

References

[1] Y. Bar-Cohen, Electroactive Polymer (EAP) Actuators as Artificial Muscles (Reality, Potential, and Challenges) (SPIE Press, Bellingham, ISBN: 9780819452979, Washington, USA, 2004).
[2] F. Carpi, D. Rossi, R. Kornbluh, R. Pelrine, P. Sommer Larsen, Amsterdam, Elsevier Science; 2008.
[3] M. Watanabe, T. Hirai, M. Suzuki, Y. Amaike Y, Appl. Phys. Lett., **74**, 2717 (1999).
[4] B. Guiffard, L. Seveyrat, G. Sebald, D. Guyomar, J. of Phys. D: Appl. Phys., **39**, 3053 (2006).
[5] Q. M. Zhang, J. Su, C. H. Kim, J. Appl. Phys. **81**, 2770 (1997).
[6] S. Eury, R. Yimnirum, V. Sundar, P. J. Moses, S. J. Jang, R.E. Newnham, Mat. Chem. And Phys., **61**, 18 (1999).
[7] F. M. Guillot, E. BalizerJ. Appl. Poly. Sci, **89**, 399 (2003).
[8] C.-W. Nan, Y. Shen, J. Ma, Annu. Rev. Mater. Res, **40,** 131 (2010).
[9] K. Wongtimnoi, B. Guiffard, A. Bogner-Van de Moortèle, L. Seveyrat, C. Gauthier C., J.-Y. Cavaillé, Comp Sci. Techn., **71**, 885 (2011).
[10] C. Park, J. H. Kang, J. S. Harrison, R. C. Costen, S. E. Lowther, Adv. Mater. **20**, 2074 (2008).
[11] S. Zhang, J. H. Kang, C. Huang, K. Ren, Q. Zhang; Advanced Materials, **17**(15), 1897 (2005).
[12] B. Guiffard, D. Guyomar, L. Seveyrat, Y. Chowanek, M. Bechelany, D. Cornu, P. Miele., J. Phys. D: App. Phys., **42**, 055503 (2009).
[13] L. Seveyrat, A. Chalkha, D Guyomar, L. Lebrun, Journal of Applied Physics, **111**(10), 104904 (2012).
[14] C. W. Nan, Progr. Mat. Sci., **37**, 1 (1993).
[15] Q. Chen, P. Du, L. Jin, W. Weng, G. Han, App. Phys. Lett., **91**, 022912 (2007).
[16] J. P. Straley, S. W. Kenkel, Phys. Rev. B, **29**, 6299 (1994).
[17] D. Stauffer, Introduction to percolation theory, Taylor and Francis, London and Philadelphia, 1985.
[18] L. Flandin, M. Verdier, B. Boutherin, Y. Brechet, J. Y. Cavaillé, Journal of Polymer Science Part B: Polymer Physics, **37**, 805 (1999).

*Corresponding author: laurence.seveyrat@insa-lyon.fr